Sensitivity of Chemistry-Transport Model Simulations to the Duration of Chemical and Transport Operators: A Case Study with GEOS-Chem v10-01

S. Philip[1,*], R. V. Martin[1, 2] and C. A. Keller[3]

[1]Department of Physics and Atmospheric Science, Dalhousie University, Halifax, Nova Scotia, Canada

[2]Harvard-Smithsonian Center for Astrophysics, Cambridge, Massachusetts, USA

[3]School of Engineering and Applied Sciences, Harvard University, Cambridge, Massachusetts, USA

* Corresponding author: Sajeev Philip, Department of Physics and Atmospheric Science, Dalhousie University, Halifax, NS, B3H 4R2, Canada (philip.sajeev@dal.ca)

Abstract

Chemistry-transport models involve considerable computational expense. Fine temporal resolution offers accuracy at the expense of computation time. Assessment is needed of the sensitivity of simulation accuracy to the duration of chemical and transport operators. We conduct a series of simulations with the GEOS-Chem chemistry-transport model at different temporal and spatial resolutions to examine the sensitivity of simulated atmospheric composition to operator duration. Subsequently, we compare the species simulated with operator durations from 10 min to 60 min as typically used by global chemistry-transport models, and identify the operator durations that optimize both computational expense and simulation accuracy. We find that longer transport

operator duration increases concentrations of emitted species such as nitrogen oxides and carbon monoxide since a more homogeneous distribution reduces loss through chemical reactions and dry deposition, depending on the chemical regime. The increased concentrations of ozone precursors increase ozone production at longer transport operator duration. Longer chemical operator duration decreases sulfate and ammonium but increases nitrate due to feedbacks with in-cloud sulfur dioxide oxidation and aerosol thermodynamics. The simulation duration decreases by up to a factor of 5 from fine (5 min) to coarse (60 min) operator duration. We assess the change in simulation accuracy with resolution by comparing the root mean square difference in ground-level concentrations of nitrogen oxides, secondary inorganic aerosols, ozone and carbon monoxide with a finer temporal or spatial resolution taken as "truth". Relative simulation error for these species increases by more than a factor of 5 from the shortest (5 min) to longest (60 min) operator duration. Chemical operator duration twice that of the transport operator duration offers more simulation accuracy per unit computation. However, relative simulation error from coarser spatial resolution generally exceeds that from longer operator duration; e.g. degrading from 2^o x 2.5^o to 4^o x 5^o increases error by an order of magnitude. We recommend prioritizing fine spatial resolution before considering different operator durations in offline chemistry-transport models. We encourage chemistry-transport model users to specify in publications the durations of operators due to their effects on simulation accuracy.

1 Introduction

Global and regional chemistry-transport models (CTMs) have a wide range of applications in studies of climate, air quality, and biogeochemical cycling. The last few decades have witnessed rapid development of modeling sophistication to tackle these issues, but that development is associated with increasing computational expense. Typically, Eulerian models divide the

47 atmosphere into numerous (10^4-10^8) grid boxes and solve the mass continuity equation to simulate
48 atmospheric composition. The concentrations of simulated species are sensitive to the duration of
49 operators (e.g., chemistry, transport) used in the CTM. Attention is needed to understand how
50 operator duration affects model performance.

51 Numerous studies have examined the sensitivity of simulations to grid resolution for ozone (Jang
52 et al., 1995; Esler et al., 2004; Ito et al., 2009; Yu et al., 2016), ozone production efficiency (Liang
53 and Jacobson 2000), and ozone sensitivity to precursor emissions (Cohan et al., 2006; Henderson
54 et al., 2010). Simulation error increases proportional to the size of the horizontal grid (Wild and
55 Prather, 2006; Prather et al., 2008). Biases can be reduced by simulating sub grid scale processes
56 such as emission plumes from point sources (Sillman et al., 1990; Valin et al., 2011), aircraft
57 exhaust (Kraabøl et al., 2002), ship exhaust (Vinken et al., 2011), mineral dust emissions (Ridley
58 et al., 2013), and lightning (Cooper et al., 2014). The spatial and temporal resolution of the
59 meteorological fields used in CTMs can also influence model processes (Bian et al., 2009). The
60 spatiotemporal variation of carbon monoxide is better represented with finer grid resolution (Wang
61 et al., 2004; Chen et al., 2009; Yan et al., 2014). Moreover, fine horizontal resolution is important
62 for air quality exposure assessment and health impact studies (Punger and West, 2013; Fountoukis
63 et al., 2013; Thompson et al., 2014; Li et al., 2015). Fine vertical resolution can better represent
64 convection (Rind et al., 2007; Arteta et al., 2009). Simulations are also sensitive to operator
65 durations (Mallet et al., 2007; Santillana et al., 2016), however, few studies have examined this
66 sensitivity.

67 CTMs solve the continuity equation for tens to hundreds of chemical species, each with number
68 density n, for individual grid boxes defined in the Eulerian model.

69 $$\frac{\partial n}{\partial t} = -\nabla \cdot nU + P - L \quad (1)$$

70 $\partial n/\partial t$ represents the local temporal evolution of n. $-\nabla \cdot nU$ represents the transport flux divergence
71 term, where U is the wind velocity vector. P and L are the local production and loss terms
72 respectively. Typically, the above equation is discretized in space, and the continuity equation is
73 simulated as a system of coupled non-linear partial differential equations with chemical and
74 transport operators. These chemical and transport operators are usually simulated sequentially
75 through operator splitting to increase computational efficiency (Hundsdorfer and Verwer, 2003).
76 The transport operator involves solving the 3-D advection equation using efficient numerical
77 schemes (Prather, 1986; Lin and Rood, 1996). The chemical operator representing the temporal
78 evolution of local sources and sinks involves numerically solving a system of coupled ordinary
79 differential equations using efficient solvers (Jacobson and Turco, 1994; Damian et al., 2002). The
80 integration timestep in a differential equation solver is important for efficient and accurate solution
81 (Jacobson and Turco, 1994). Moreover, the model accuracy is affected by the duration of chemical
82 and transport operators (Mallet and Sportisse, 2006; Mallet et al., 2007), and the order in which
83 these operators are applied (Sportisse, 2000; Santillana et al., 2016). The operator splitting method
84 requires the coupling between individual operators to be negligible over the operator duration.
85 However, reducing operator durations increases computational expense. Attention is needed to this
86 tradeoff.

87 We examine the sensitivity of a CTM to operator duration by conducting a series of simulations at
88 different horizontal resolutions and operator durations. We then identify the optimal operator
89 duration from the range of operator durations from 10 min to 60 min usually used by global CTMs
90 (e.g., Horowitz et al., 2003; Huijnen et al. 2010). Section 2 describes the sensitivity simulations,
91 the method to quantify the simulation error, as well as the method to identify the simulation
92 operator durations that best account for both computational expense and simulation accuracy.

Comparison of the sensitivity simulations, description of resolution-dependent errors, and the identification of appropriate chemical and transport operator durations are examined in section 3.

2 Materials and Methods

2.1 GEOS-Chem simulations

We conduct a series of sensitivity simulations with the GEOS-Chem CTM (version 10-01; www.geos-chem.org) at different horizontal resolutions and operator durations to examine the individual sensitivities to chemical and transport operator durations. The GEOS-Chem model (Bey et al., 2001) is used by about 100 research groups worldwide to simulate the oxidant-aerosol system. GEOS-Chem has the capability to be driven with several generations of assimilated meteorological data from the Goddard Earth Observing System (GEOS) at the NASA Global Modeling Assimilation Office (GMAO). For computational expedience, GEOS-Chem global simulations are often conducted using horizontal resolutions of either 4^o x 5^o or 2^o x 2.5^o degraded from the native resolution of GEOS meteorology. GEOS-Chem also has the capability for nested regional simulations where the global model provides dynamic boundary condition to the regional grids (Wang et al., 2004; Chen et al., 2009; Zhang et al., 2011; van Donkelaar et al., 2012). We use the GEOS-5 (or GEOS-5.2.0) meteorology available at a native horizontal resolution of 0.5^o x 0.667^o (Rienecker et al., 2008). It includes three-hour averaged 2-D fields such as mixed layer depth, and six-hour averaged 3-D fields such as zonal and meridional wind, and convective mass flux. The height of the lowest level of the model is approximately 130 meters above the sea level, with 47 vertical levels.

GEOS-Chem performs species advection (A), vertical mixing (V), cloud convection (Z) and wet deposition (W) for every transport operator duration (T), as well as dry deposition (D), emissions

115 (E), photolysis (P), and chemistry (G) for every chemical operator duration (C) in the following
116 order,

117 $$A(T) \cdot D(C) \cdot E(C) \cdot V(T) \cdot Z(T) \cdot P(C) \cdot G(C) \cdot W(T) \quad (2)$$

118 The traditional transport operator durations are 30 minutes at 4^o x 5^o resolution, 15 minutes at 2^o
119 x 2.5^o resolution, and 10 min at 0.5^o x 0.67^o resolution. The traditional chemical operator durations
120 have varied from either 60 min or twice the transport operator duration based on the Strang
121 operator splitting scheme (Strang, 1968) which follows $T \cdot C \cdot T \cdot T \cdot C \cdot T$ order repetitively with
122 $C = 2 \times T$. Transport operations are repeated twice before a chemical operation when $C = 2 \times T$.
123 We also test an alternate splitting scheme which follows $T \cdot C \cdot T \cdot C$ order repetitively with $C =$
124 T.

125 Advection is based on the multi-dimensional flux-form semi-Lagrangian advection scheme (Lin
126 and Rood, 1996; Lin et al., 1994), with an additional pressure-fixer algorithm implemented for the
127 conservation of species mass (Rotman et al., 2004). Transport by convection is coupled (Balkanski
128 et al., 1993; Wu et al., 2007) with gas-aerosol wet deposition (Liu et al., 2001; Wang et al., 2011;
129 Amos et al., 2012). GEOS-Chem uses an internal integration timestep of 5 min for convective
130 mixing. We use a non-local boundary layer mixing scheme for vertical transport (Holtslag and
131 Boville, 1993, Lin and McElroy, 2010).

132 Emissions are processed through the HEMCO module (Keller et al., 2014). A resistance-in-series
133 method is used for dry deposition of species (Wesely, 1989; Wang et al., 1998; Zhang et al., 2001;
134 Fisher et al., 2011).

135 GEOS-Chem uses a Sparse Matrix Vectorized GEAR II chemistry solver (Jacobson and Turco,
136 1994; Jacobson, 1995; 1998). The oxidant-aerosol chemistry simulation includes organic and black

carbon (Park et al., 2003), mineral dust (Fairlie et al., 2007; Zender et al., 2003; Ginoux et al., 2001), sea salt (Alexander et al., 2005; Jaegle et al., 2011), and the sulfate-nitrate-ammonium system (Park et al., 2004). The photolysis frequency is calculated (Mao et al., 2010; Eastham et al., 2014) at the middle of the chemical operator duration using the Fast-JX algorithm (Bian and Prather, 2002). Simulation of gas-aerosol interactions are performed by aerosol extinction effects on photolysis rates (Martin et al., 2003), and heterogeneous chemistry (Jacob, 2000) including aerosol uptake of N_2O_5 (Evans and Jacob, 2005) and HO_2 (Mao et al., 2013). The ISORROPIA II thermodynamic module (Fontoukis and Nenes, 2007) performs aerosol-gas partitioning (Pye et al., 2009).

We conduct simulations for 2010 July at two horizontal resolutions of 4^o x 5^o and 2^o x 2.5^o globally, and 0.5^o x 0.667^o over the North America (140^oW–40^oW, 10^oN–70^oN) and East Asia (70^oW–150^oW, 11^oS–55^oN) nested regions. We use the 4^o x 5^o global simulation to archive dynamic boundary conditions every three hours for the nested simulations. We use one month spin up with each GEOS-Chem simulation to reduce the influence of initial conditions.

2.2 Computing platform

We conduct all simulations on the same computing platform to compare their computational performance. We use the Glooscap cluster of the Atlantic Computational Excellence Network (ACENET) Consortium of Canadian Universities (http://www.ace-net.ca/wiki/Glooscap). The operating system is Linux 4.8. We use Intel Fortran compiler version 12. Each GEOS-Chem simulation is submitted as a 16-thread parallelized job on a single node.

We calculate the CPU time for the month of July for each operator separately using the Fortran-intrinsic routine, CPU_TIME. We found this value identical to the one calculated using the Linux

command 'qacct –j'. To reduce the effects of other jobs on the shared cluster, we repeat simulations five times, while excluding data output operations to minimize sensitivity to system input/output, and use the median to represent CPU time.

2.3 Assessing the relative simulation error

We treat the simulation with the shortest operator duration as the most accurate. This approach exploits the reduction in error associated with coupling across operators as operator duration diminishes. Assessing simulation error versus operator duration through comparison with observations is impaired by imperfect model processes, by the sparseness of measurements, and by model-observation representativeness biases. We take as "truth" the concentrations simulated with a chemical operator duration (C) of 10 minutes and a transport operator duration (T) of 5 minutes (represented as C10T05). Finer resolutions are computationally prohibitive. We define the relative simulation error E^s_{sim} for species *s* as the root mean square error (RMSE) of the species concentrations simulated with the finest resolution ("truth") and the simulation under consideration (*Sim*), normalized by the concentrations in simulation "truth",

$$E^s_{sim} = \frac{\sqrt{N}\sqrt{\sum_{i=1}^{i=N}(Truth_i^s - Sim_i^s)^2}}{\sum_{i=1}^{i=N} Truth_i^s} \quad (3)$$

where, *i* represents a particular grid box, with a total number of *N* grid boxes of interest. RMSE in the numerator is chosen instead of absolute difference to more heavily penalize extrema. Normalization with the mass of the "true" simulation is intended to cross-compare E^s_{sim} of different species. E^s_{sim} captures the variation of a species *s* from the "true" simulation.

Here, we focus on four key species relevant to atmospheric chemistry, namely nitrogen oxides ($NO_x = NO + NO_2$), secondary inorganic aerosols (SIA: sum of sulfate, nitrate and ammonium), ozone (O_3), and carbon monoxide (CO). These species represent a range of lifetimes from a day (NO_x) to weeks (CO). The focus on SIA is designed to devote more attention to chemically active species than to mineral dust and sea salt. We sample the instantaneous values of simulated ground-level concentrations of these atmospheric species every 60 min to span the diurnal variation of chemical environments. We focus on concentrations in July near the Earth's surface when and where chemical and transport timescales tend to be short.

2.4 Identifying the optimal operator duration

A practical way to select optimal chemical and transport operator durations is to identify the simulation with the lowest error (E^s_{sim}) per unit of computation time. To quantify the simulation accuracy per unit CPU time, we propose a simple metric, the CPU-time adjusted Composite Normalized Error (CNE) which represents a tradeoff between the simulation accuracy, and the associated computation expense. This is performed by normalizing the relative simulation error E^s_{sim} for species s by the CPU time t for the simulation under consideration t_{sim} and for a reference simulation t_{ref}, and taking the mean of four species.

$$CNE = \left(\frac{1}{4} \times \sum_s \frac{E^s_{sim}}{E^s_{ref}} \right) \times \left(\frac{t_{sim}}{t_{ref}} \right) \quad (4)$$

We normalize E^s_{sim} by the reference E^s_{ref} so that the CPU-time adjusted Composite Normalized Error for each species is of similar magnitude. The variation of CNE across operator durations is unaffected by the choice of reference simulation; C10T10 used here. The relative value of CPU

200 time versus simulation accuracy is subjective and depends on scientific objective. This definition
201 of CNE gives equal weighting to the respective cost of CPU time and simulation accuracy. The
202 simulation with the lowest CNE is used to identify an optimal chemical and transport operator
203 duration.

204 **3 Results and discussion**

205 Figure 1 shows the computational performance for the series of GEOS-Chem simulations
206 conducted here. The CPU time decreases by factors of 3-5 from fine to coarse operator duration.
207 The CPU time increases by about a factor of 4 from 4^o x 5^o to 2^o x 2.5^o and another factor of 2 to a
208 single nested simulation at 0.5^o x 0.667^o. This linearity implies that grid boxes are sufficiently large
209 that CPU time is proportional to the number of grid boxes, and that transport integration timesteps
210 constrained by the Courant-Freidrich-Lewy criterion (Courant et al., 1967) are largely unaffected
211 by changes to grid box size at these resolutions. Comparison of individual CPU times for chemical
212 and transport operators shows that performing a single cycle of all chemical operations takes ~4
213 times that of a single cycle of transport operations at the global scale. This factor is reduced for
214 nested simulations due in part to the additional CPU time for simulating boundary conditions.

215 Figure 2 illustrates the sensitivity of the simulations to chemical and transport operators at 2^o x
216 2.5^o horizontal resolution. The left column shows the species concentrations for the "true"
217 simulation (C10T05). The middle column shows the difference in species concentrations from
218 doubling the transport operator duration. Increasing the transport operator duration tends to
219 increase concentrations of emitted species like CO and NO_x over source regions since species are
220 more uniformly mixed by long operator durations before loss processes such as deposition and
221 chemistry occur. More homogeneous fields have lower dry deposition rates as a larger fraction is

222 mixed aloft, and lower chemical loss rates depending on the chemical regime. The increase in CO
223 over source regions is partly associated with decreases in OH. Increasing concentrations of ozone
224 precursors increases ozone production ($P[O_3]$). Wild and Prather (2006) similarly found that ozone
225 production increases at coarser horizontal resolution. Increasing the transport operator duration
226 increases SIA components, especially over the source regions of East Asia, North India, and North
227 America.

228 The right column in Fig. 2 shows the change in species concentrations from increasing the
229 chemical operator duration. Hydroxyl radical concentrations increase, NO_x concentrations
230 decrease, and $P[O_3]$ decreases with increasing chemical operator durations over source regions.
231 Berntsen and Isaken (1997) found that the error introduced by coarser chemical operator durations
232 is higher in polluted regions than the clean background due to the increased time lag, and invariant
233 production and loss across rapid chemical cycles. A longer chemical operator duration decreases
234 sulfate and ammonium but increases nitrate over source regions. Inspection of SO_2 and H_2O_2 fields
235 indicates that sulfate formation through H_2O_2 in clouds decreases at longer chemical operator
236 durations. In turn, SO_2 and NH_3 concentrations increase at longer chemical operator durations due
237 to the corresponding decreases in ammonium sulfate or ammonium bisulfate. The additional free
238 ammonia at longer chemical operator durations tends to promote regional ammonium nitrate
239 formation depending on local thermodynamics. An increase of total SIA mass with the increasing
240 chemical operator duration is driven by nitrate and ammonium, and partially compensated by a
241 reduction in sulfate, especially downwind of source regions. We find similar spatial patterns for
242 other operator duration combinations, and other horizontal resolutions.

243 Figure 3 shows the sensitivity of simulated species to changes in operator duration (C20T10 to
244 C10T05) at two other horizontal resolutions (global 4^o x 5^o, and nested North America 0.5^o x 0.67^o

245 simulations) considered here. Spatial patterns of monthly mean ground-level concentrations, and
246 absolute differences are similar, albeit with finer spatial heterogeneity resolved in the nested
247 simulation. However, some resolution dependent differences do arise reflecting nonlinear
248 feedbacks.

249 Figures 4 shows the relative simulation error for nitrogen oxides, secondary inorganic aerosols,
250 ozone and carbon monoxide with varying operator durations at 2^o x 2.5^o horizontal resolution.
251 Relative simulation errors for all these major species increase by more than a factor of 5 from the
252 shortest to longest operator duration. Errors increase fairly smoothly with increasing chemical and
253 transport operator duration until the transport operator duration exceeds 30 min. Then errors
254 increase by an order of magnitude for long lived species of O_3 and CO. Relative simulation errors
255 for other horizontal resolutions follows similar pattern. These relative errors are comparable to
256 typical model-observation errors of ~30% for NO_x (Boersma et al., 2008; Hudman et al., 2006)
257 and 20 - 40% for SIA (Philip et al., 2014; Heald et al., 2012), while smaller than typical model-
258 observation errors of ~20% for ozone (Zhang et al., 2011; Wang et al., 2009) and 10 - 20% for CO
259 (Duncan et al., 2007; Shindell et al., 2006).

260 Figure 5 shows the difference in simulated species at 2^o x 2.5^o horizontal resolution for the GEOS-
261 Chem traditional (C30T15) minus the finest operator durations considered (C10T05). The spatial
262 variation for the monthly mean ground-level concentrations is generally within 5-15% for short
263 lived species like NO_x and SIA, and within 1% for longer lived species like O_3 and CO. Santillana
264 et al. (2016) similarly found an upper limit of 10% for operator splitting errors. However, the
265 maximum hourly spatial variation can exceed 50% for short lived species and 5% for longer lived
266 species. The spatial pattern of extrema resembles that of the monthly mean, albeit with more
267 heterogeneity from synoptic variation.

We also examined the diurnal variation and vertical profile of extrema. Extrema arise from all times of day with a slight tendency for larger values for NO_x at night, for ozone near sunrise and sunset, and for SIA and CO near noon. Zonal mean vertical profiles exhibit largest differences in the lower troposphere for NO_x and SIA, with more homogeneous differences throughout the troposphere for O_3 and CO. Near the subtropical jets of the upper troposphere O_3 and CO have maximum extrema of up to 3%.

Figure 6 shows the CPU-time adjusted Composite Normalized Error for the GEOS-Chem simulations at various horizontal resolutions and operator durations. The CNE is significantly higher with C = T than C = 2 x T. We confirmed this tendency with different choices of "truth" (such as C05T05, C10T10) or reference (such as C10T05) simulations. This finding motivates the traditional approach of using C = 2 x T in GEOS-Chem simulations. Applying the chemical operator as frequently as the transport operator (with C = T) appears to increase computation cost with little benefit in accuracy. The CNE for all three horizontal resolutions have noisy minima with a chemical operator duration of 20 min and a transport operator duration of 10 min (C20T10). A unit of computation time has a similar efficiency for a small range of operator durations from 10 min to 20 min. We found similar patterns in the variation of CNE with operator durations with CNE calculated for selected domains, such as over Northern Hemisphere, nested model regions, land grid boxes, and over the entire troposphere. We conducted additional simulations at 4^o x 5^o horizontal resolution for January 2011 with a spin up of 7 months, and found similar patterns in CNE.

The relative simulation error decreases by 40-50% (Fig. 4) by changing the operator duration from the traditional (C30T15) to the optimal (C20T10) at 2^o x 2.5^o horizontal resolution. The relative

290 spatial variations are <20% for NO_x and SIA, and <1% for O_3 and CO. However, the CPU time
291 increases by 20% by the decrease in operator duration.

292 Table 1 shows the relative simulation error at 4^o x 5^o horizontal resolution with "truth" at 2^o x 2.5^o
293 resolution (C10T05) to investigate the tradeoff between horizontal resolution and operator
294 duration. The simulation error for all species at 4^o x 5^o resolution increases by an order of
295 magnitude compared to 2^o x 2.5^o resolution for any choice of operator duration tested here. The
296 error in this configuration is insensitive to operator duration, and dominated by representativeness
297 differences due to spatial structure resolved at 2^o x 2.5^o resolution, but not at 4^o x 5^o resolution.
298 Nonlinear chemistry at different horizontal resolutions (e.g., Wild and Prather, 2006) also plays a
299 role. Numerical errors due to advection processes generally exceed those from operator splitting
300 (e.g., Prather et al., 2008; Santillana et al., 2016). We therefore recommend prioritizing horizontal
301 resolution over operator duration for offline CTMs using time-averaged meteorological fields as
302 tested here. As meteorological fields used in CTMs become available at finer temporal and spatial
303 resolution, the value of shorter operator duration should further increase. We encourage the CTM
304 users to specify the durations of operators in publications due to its effect on simulation accuracy.

305 **4 Conclusions**

306 The computational expense of chemistry-transport models warrants investigation into their
307 efficiency and accuracy. Solving the continuity equation in CTMs through operator splitting
308 method offers numerical efficiency, however, few studies have examined the implications of
309 operator duration on simulation accuracy. We conducted simulations with the GEOS-Chem model
310 for multiple choices of operator duration from 10 min to 60 min as typically used by global CTMs.
311 We found that longer transport operator durations increase ozone precursors and ozone production

312 over source regions since a more homogeneous distribution reduces loss through chemical
313 reactions and dry deposition. Longer chemical operator durations decrease NO_x and ozone
314 production over source regions. Longer chemical operator durations reduce sulfate and ammonium
315 concentrations, however increase nitrate due to feedbacks with in-cloud SO_2 oxidation and local
316 aerosol thermodynamics.

317 We investigated the computational efficiency with the GEOS-Chem model, and found that the
318 simulation computation time decreases by up to a factor of 5 from fine (C10T05) to coarse
319 (C60T60) operator duration. The chemical operator consumes about four times the CPU time of
320 the transport operator. We subsequently compared the root mean square differences in the ground-
321 level concentrations of nitrogen oxides, secondary inorganic aerosols, ozone and carbon monoxide
322 with a finer temporal or spatial resolution taken as "truth", and estimated the relative simulation
323 error. The relative simulation error for these species increases by more than a factor of 5 from the
324 shortest to longest operator duration.

325 In order to account for simulation accuracy with computational cost, we proposed a metric, CPU-
326 time adjusted Composite Normalized Error that identifies the operator duration with respect to
327 CPU cost. We recommend the approach of using C = 2 x T for all horizontal resolutions. The CNE
328 exhibits a noisy minimum for a chemical operator duration of 20 min and transport operator
329 duration of 10 min for the range of operator durations and horizontal resolutions considered here.
330 Nonetheless, the relative simulation error from changing horizontal resolution exceeds that from
331 changing operator durations within a horizontal resolution. We recommend prioritizing fine spatial
332 resolution before considering different operator durations in offline CTMs with time-averaged
333 archived meteorological fields as tested here. The importance of shorter operator durations should
334 increase with the availability of time-averaged meteorological fields at higher temporal resolution.

Short operator durations could offer even greater benefits to simulation accuracy in online CTMs that offer meteorological fields at temporal resolutions closer to operator duration. We encourage the CTM users to specify in publications the durations of operators due to their effects on simulation accuracy.

Code Availability

The GEOS-Chem code is freely accessible to the public, by following the guidelines in http://wiki.geos-chem.org/). This work used GEOS-Chem version 10-01.

Acknowledgements

This work was supported by NSERC and ACENET. We thank Colette Heald, Daniel Jacob and Patrick Kim for useful comments at the early stages of this research. We are grateful to two anonymous reviewers for helpful comments.

References

Alexander, B., Park, R. J., Jacob, D. J., Li, Q. B., Yantosca, R. M., Savarino, J., Lee, C. C. W. and Thiemens, M. H.: Sulfate formation in sea-salt aerosols: Constraints from oxygen isotopes, J. Geophys. Res., 110, D10307, doi:10.1029/2004JD005659, 2005.

Amos, H. M., Jacob, D. J., Holmes, C. D., Fisher, J. A., Wang, Q., Yantosca, R. M., Corbitt, E. S., Galarneau, E., Rutter, A. P., Gustin, M. S., Steffen, A., Schauer, J. J., Graydon, J. A., St Louis, V. L., Talbot, R. W., Edgerton, E. S., Zhang, Y., and Sunderland, E. M.: Gas-particle partitioning of atmospheric Hg(II) and its effect on global mercury deposition, Atmos. Chem. Phys., 12, 591-603, doi:10.5194/acp-12-591-2012, 2012.

Arteta, J., Marecal, V., and Riviere, E. D.: Regional modelling of tracer transport by tropical convection – Part 2: Sensitivity to model resolutions, Atmos. Chem. Phys., 9, 7101-7114, doi:10.5194/acp-9-7101-2009, 2009.

Balkanski, Y. J., Jacob, D. J., Gardner, G. M., Graustein, W. C., and Turekian, K. K.: Transport and residence times of tropospheric aerosols inferred from a global three-dimensional simulation of ^{210}Pb, J. Geophys. Res., 98, 20573-20586, doi:10.1029/93JD02456, 1993.

Berntsen, T. K., and Isaksen, I. S. A.: A global three-dimensional chemical transport model for the troposphere: 1. Model description and CO and ozone results, J. Geophys. Res., 102, 21239-21280, doi:10.1029/97JD01140, 1997.

Bey, I., Jacob, D. J., Yantosca, R. M., Logan, J. A., Field, B. D., Fiore, A. M., Li, Q. B., Liu, H. G. Y., Mickley, L. J., and Schultz, M. G.: Global modeling of tropospheric chemistry with assimilated meteorology: Model description and evaluation, J. Geophys. Res., 106, 23073-23095, doi:10.1029/2001JD000807, 2001.

Bian, H., Chin, M., Rodriguez, J. M., Yu, H., Penner, J. E., and Strahan, S.: Sensitivity of aerosol optical thickness and aerosol direct radiative effect to relative humidity, Atmos. Chem. Phys., 9, 2375-2386, doi:10.5194/acp-9-2375-2009, 2009.

Bian, H., and Prather, M. J.: Fast-J2: Accurate simulation of stratospheric photolysis in global chemical models, J. Atmos. Chem., 41, 281-296, doi:10.1023/A:1014980619462, 2002.

Boersma, K. F., Jacob, D. J., Eskes, H. J., Pinder, R. W., Wang, J., and van der A, R. J.: Intercomparison of SCIAMACHY and OMI tropospheric NO_2 columns: Observing the diurnal evolution of chemistry and emissions from space, J. Geophys. Res., 113, D16S26, doi:10.1029/2007JD008816, 2008.

Chen, D., Wang, Y., McElroy, M. B., He, K., Yantosca, R. M., and Le Sager, P.: Regional CO pollution and export in China simulated by the high-resolution nested-grid GEOS-Chem model, Atmos. Chem. Phys., 9, 3825-3839, 10.5194/acp-9-3825-2009, 2009.

Cohan, D. S., Hu, Y., and Russell, A. G.: Dependence of ozone sensitivity analysis on grid resolution, Atmos. Environ., 40, 126-135, doi:10.1016/j.atmosenv.2005.09.031, 2006.

Cooper, M., Martin, R. V., Wespes, C., Coheur, P., Clerbaux, C., and Murray, L. T.: Tropospheric nitric acid columns from the IASI satellite instrument interpreted with a chemical transport model: Implications for parameterizations of nitric oxide production by lightning, J. Geophys. Res.-Atmos., 119, 10068-10079, doi:10.1002/2014JD021907, 2014.

Courant, R., Friedrichs, K., and Lewy, H.: On partial difference equations of mathematical physics, IBM Journal of Research and Development, 11, 215-234, doi:10.1147/rd.112.0215, 1967.

Damian, V., Sandu, M., Potra, G. R., and Carmichael: The kinetic preprocessor KPP-a software environment for solving chemical kinetics, Comput. Chem. Eng., 26, 1567-1579, doi:10.1016/S0098-1354(02)00128-X, 2002.

Duncan, B. N., Logan, J. A. , Bey, I., Megretskaia, I. A., Yantosca, R. M., Novelli, P. C., Jones, N. B., and Rinsland, C. P.: Global budget of CO, 1988 –1997: Source estimates and validation with a global model, J. Geophys. Res., 112, D22301, doi:10.1029/2007JD008459, 2007.

Eastham, S. D., Weisenstein, D. K., and Barrett, S. R. H.: Development and evaluation of the unified tropospheric–stratospheric chemistry extension (UCX) for the global chemistry-transport model GEOS-Chem, Atmos. Environ, 89, 52-63, doi:10.1016/j.atmosenv.2014.02.001, 2014.

Esler, J. G., Roelofs, G. J., Kohler, M. O., and O'Connor, F. M.: A quantitative analysis of grid-related systematic errors in oxidising capacity and ozone production rates in chemistry transport models, Atmos. Chem. Phys., 4, 1781-1795, doi:10.5194/acp-4-1781-2004, 2004.

Evans, M. J., and Jacob, D. J.: Impact of new laboratory studies of N_2O_5 hydrolysis on global model budgets of tropospheric nitrogen oxides, ozone, and OH, Geophys. Res. Lett., 32, L09813, doi:10.1029/2005GL022469, 2005.

Fairlie, T. D., Jacob, D. J., and Park, R. J.: The impact of transpacific transport of mineral dust in the United States, Atmos. Environ., 41, 1251-1266, doi:10.1016/j.atmosenv.2006.09.048, 2007.

Fisher, J. A., Jacob, D. J., Wang, Q., Bahreini, R., Carouge, C. C., Cubison, M. J., Dibb, J. E., Diehl, T., Jimenez, J. L., Leibensperger, E. M., Lu, Z., Meinders, M. B. J., Pye, H. O. T., Quinn, P. K., Sharma, S., Streets, D. G., van Donkelaar, A., and Yantosca, R. M.: Sources, distribution, and acidity of sulfate-ammonium aerosol in the Arctic in winter-spring, Atmos. Environ., 45, 7301-7318, doi:10.1016/j.atmosenv.2011.08.030, 2011.

Fountoukis, C., Koraj, D., Denier van der Gon, H.A.C., Charalampidis, P. E., Pilinis, C., and Pandis, S. N.: Impact of grid resolution on the predicted fine PM by a regional 3-D chemical transport model, Atmos. Environ., 68, 24-32, doi:10.1016/j.atmosenv.2012.11.008, 2013.

Fountoukis, C., and Nenes, A.: ISORROPIA II: a computationally efficient thermodynamic equilibrium model for K^+-Ca^{2+}-Mg^{2+}-NH_4^+-Na^+-SO_4^{2-}-NO_3^--Cl^--H_2O aerosols, Atmos. Chem. Phys., 7, 4639-4659, doi:10.5194/acp-7-4639-2007, 2007.

Ginoux, P., Chin, M., Tegen, I., Prospero, J. M., Holben, B., Dubovik, O., and Lin, S. J.: Sources and distributions of dust aerosols simulated with the GOCART model, J. Geophys. Res., 106, 20255–20274, doi:10.1029/2000JD000053, 2001.

Heald, C. L., Collett Jr., J. L., Lee, T., Benedict, K. B., Schwandner, F. M., Li, Y., Clarisse, L., Hurtmans, D. R., Van Damme, M., Clerbaux, C., Coheur, P.-F., Philip, S., Martin, R. V., and Pye, H. O. T.: Atmospheric ammonia and particulate inorganic nitrogen over the United States, Atmos. Chem. Phys., 12, 10295-10312, doi:10.5194/acp-12-10295-2012, 2012.

Henderson, B. H., Jeffries, H. E., Kim, B. U., and Vizuete, W. G.: The influence of model resolution on ozone in industrial volatile organic compound plumes, J. Air Waste Manage. Assoc., 60, 1105–1117, doi:10.3155/1047-3289.60.9.1105, 2010.

Holtslag, A. A. M., and Boville, B. A.: Local Versus Nonlocal Boundary-Layer Diffusion in a Global Climate Model, J. Clim., 6, 1825-1842, doi:10.1175/1520-0442(1993)006<1825:LVNBLD>2.0.CO;2, 1993.

Horowitz, L. W., Walters, S., Mauzerall, D. L., Emmons, L. K., Rasch, P. J., Granier, C., Tie, X., Lamarque, J., Schultz, M. G., Tyndall, G. S., Orlando, J. J., and Brasseur, G. P.: A global simulation of tropospheric ozone and related tracers: Description and evaluation of MOZART, version 2, J. Geophys. Res., 108, 4784, doi:10.1029/2002JD002853, 2003.

Hudman, R. C.; Jacob, D. J., Turquety, S., Leibensperger, E. M., Murray, L. T., Wu, S.,Gilliland, A. B., Avery, M., Bertram, T. H., Brune, W., Cohen, R. C., Dibb, J. E., Flocke, F. M., Fried, A., Holloway, J., Neuman, J. A., Orville, R., Perring, A., Ren, X., Sachse, G. W., Singh, H. B., Swanson, A., and Wooldridge, P. J.: Surface and lightning sources of nitrogen oxides over the United States: Magnitudes, chemical evolution, and outflow, J. Geophys. Res., 112, D12S05, doi:10.1029/2006JD007912, 2007.

Huijnen, V., Williams, J., van Weele, M., van Noije, T., Krol, M., Dentener, F., Segers, A., Houweling, S., Peters, W., de Laat, J., Boersma, F., Bergamaschi, P., van Velthoven, P., Le Sager, P., Eskes, H., Alkemade, F., Scheele, R., Nédélec, P., and Pätz, H. -W.: The global chemistry transport model TM5: description and evaluation of the tropospheric chemistry version 3.0, Geosci. Model Dev., 3, 445-473, doi:10.5194/gmd-3-445-2010, 2010.

Hundsdorfer, W., and Verwer, J.: Numerical solution of time-dependent advection-diffusion-reaction equations, Springer Series in Computational Mathematics, 33, 325-417, doi:10.1007/978-3-662-09017-6_4, 2003.

Ito, A., Sillman, S., and Penner J. E.: Global chemical transport model study of ozone response to changes in chemical kinetics and biogenic volatile organic compounds emissions due to increasing temperatures: Sensitivities to isoprene nitrate chemistry and grid resolution, J. Geophys. Res., 114, D09301, doi:10.1029/2008JD011254, 2009.

Jacob, D.: Heterogeneous chemistry and tropospheric ozone, Atmos. Environ., 34, 2131-2159, doi:10.1016/S1352-2310(99)00462-8, 2000.

Jacobson, M. Z.: Computation of global photochemistry with SMVGEAR II, Atmos. Environ., 29, 2541-2546, doi:10.1016/1352-2310(95)00194-4, 1995.

Jacobson, M. Z.: Improvement of SMVGEAR II on vector and scalar machines through absolute error tolerance control, Atmos. Environ., 32, 791-796, doi:10.1016/S1352-2310(97)00315-4, 1998.

Jacobson, M., and Turco, R. P.: SMVGEAR - A SPARSE-MATRIX, VECTORIZED GEAR CODE FOR ATMOSPHERIC MODELS, Atmos. Environ., 28, 273-284, doi:10.1016/1352-2310(94)90102-3, 1994.

Jaegle, L., Quinn, P. K., Bates, T. S., Alexander, B., and Lin, J.-T.: Global distribution of sea salt aerosols: new constraints from in situ and remote sensing observations, Atmos. Chem. Phys., 11, 3137-3157, doi:10.5194/acp-11-3137-2011, 2011.

Jang, J. C., Jeffries, H. E., and Tonnesen, S.: Sensitivity of ozone to model grid resolution - II. Detailed process analysis for ozone chemistry, Atmos. Environ., 29, 3101-3114, doi:10.1016/1352-2310(95)00119-J, 1995.

Keller, C. A., Long, M. S., Yantosca, R. M., Da Silva, A. M., Pawson, S., and Jacob, D. J.: HEMCO v1.0: a versatile, ESMF-compliant component for calculating emissions in atmospheric models, Geosci. Model Dev., 7, 1409-1417, doi:10.5194/gmd-7-1409-2014, 2014.

Kraabøl, A. G., Berntsen, T. K., Sundet, J. K., and Stordal, F.: Impacts of NO_x emissions from subsonic aircraft in a global three-dimensional chemistry transport model including plume processes, J. Geophys. Res., 107, 4655, doi:10.1029/2001JD001019, 2002.

Li, Y., Henze, D. K., Jack, D., and Kinney, P.: The influence of air quality model resolution on health impact assessment for fine particulate matter and its components, Air Qual., Atmos. Health, 1-18, doi:10.1007/s11869-015-0321-z, 2015.

Liang, J., and Jacobson, M. Z.: Effects of subgrid segregation on ozone production efficiency in a chemical model, Atmos. Environ., 34, 2975-2982, doi:10.1016/S1352-2310(99)00520-8, 2000.

Lin, J., and McElroy, M. B.: Impacts of boundary layer mixing on pollutant vertical profiles in the lower troposphere: Implications to satellite remote sensing, Atmos. Environ., 44, 1726-1739, doi:10.1016/j.atmosenv.2010.02.009, 2010.

Lin, S., and Rood, R. B.: Multidimensional Flux-Form Semi-Lagrangian Transport Schemes, Mon. Weather Rev., 124, 2046-2070, doi:10.1175/1520-0493(1996)124<2046:MFFSLT>2.0.CO;2, 1996.

Lin, S., Chao, W. C., Sud, Y. C., and Walker, G. K.: A Class of the van Leer-type Transport Schemes and Its Application to the Moisture Transport in a General Circulation Model, Mon. Weather Rev., 122, 1575-1593, doi:10.1175/1520-0493(1994)122<1575:ACOTVL>2.0.CO;2, 1994.

Liu, H. Y., Jacob, D. J., Bey, I., and Yantosca, R. M.: Constraints from Pb-210 and Be-7 on wet deposition and transport in a global three-dimensional chemical tracer model driven by assimilated meteorological fields, J. Geophys. Res., 106, 12109-12128, doi:10.1029/2000JD900839, 2001.

Mallet, V. and Sportisse, B.: Uncertainty in a chemistry-transport model due to physical parameterizations and numerical approximations: An ensemble approach applied to ozone modeling, J. Geophys. Res., 111, D01302, doi:10.1029/2005JD006149, 2006.

Mallet, V., Pourchet, A., Quélo, D., and Sportisse, B.: Investigation of some numerical issues in a chemistry-transport model: Gas-phase simulations, J. Geophys. Res., 112, D15301, doi:10.1029/2006JD008373, 2007.

Mao, J., Jacob, D. J., Evans, M. J., Olson, J. R., Ren, X., Brune, W. H., St Clair, J. M., Crounse, J. D., Spencer, K. M., Beaver, M. R., Wennberg, P. O., Cubison, M. J., Jimenez, J. L., Fried, A., Weibring, P., Walega, J. G., Hall, S. R., Weinheimer, A. J., Cohen, R. C., Chen, G., Crawford, J. H., McNaughton, C., Clarke, A. D., Jaegle, L., Fisher, J. A., Yantosca, R. M., Le Sager, P., and Carouge, C.: Chemistry of hydrogen oxide radicals (HO_x) in the Arctic troposphere in spring, Atmos. Chem. Phys., 10, 5823-5838, doi:10.5194/acp-10-5823-2010, 2010.

Mao, J., Fan, S., Jacob, D. J., and Travis, K. R.: Radical loss in the atmosphere from Cu-Fe redox coupling in aerosols, Atmos. Chem. Phys., 13, 509-519, doi:10.5194/acp-13-509-2013, 2013.

Martin, R. V., Jacob, D. J., Yantosca, R. M., Chin, M., and Ginoux, P.: Global and regional decreases in tropospheric oxidants from photochemical effects of aerosols, J. Geophys. Res., 108, 4097, doi:10.1029/2002JD002622, 2003.

Park, R. J., Jacob, D. J., Chin, M., and Martin, R. V.: Sources of carbonaceous aerosols over the United States and implications for natural visibility, J. Geophys. Res.-Atmos., 108, 4355, doi:10.1029/2002JD003190, 2003.

Park, R. J., Jacob, D. J., Field, B. D., Yantosca, R. M., and Chin, M.: Natural and transboundary pollution influences on sulfate-nitrate-ammonium aerosols in the United States: Implications for policy, J. Geophys. Res.-Atmos., 109, D15204, doi:10.1029/2003JD004473, 2004.

Philip, S., Martin, R.V., van Donkelaar, A., Lo, J. W.-H., Wang, Y., Chen, D., Zhang, L., Kasibhatla, P. S., Wang, S. W., Zhang, Q., Lu, Z., Streets, D. G., Bittman, S., and Macdonald, D. J.: Global chemical composition of ambient fine particulate matter for exposure assessment, Environ. Sci. Technol., 48, 13060-13068, doi:10.1021/es502965b, 2014.

Prather, M. J.: Numerical advection by conservation of second-order moments, J. Geophys. Res., 91, 6671-6681, doi:10.1029/JD091iD06p06671, 1986.

Prather, M. J., Zhu, X., Strahan, S. E., Steenrod, S. D., and Rodriguez, J. M.: Quantifying errors in trace species transport modeling, Proc. Natl. Acad. Sci. U. S. A., 105, 19617-19621, doi:10.1073/pnas.0806541106, 2008.

Punger, E. M., and West, J. J.: The effect of grid resolution on estimates of the burden of ozone and fine particulate matter on premature mortality in the USA, Air Qual., Atmos. Health, 6, 563-573, doi:10.1007/s11869-013-0197-8, 2013.

Pye, H. O. T., Liao, H., Wu, S., Mickley, L. J., Jacob, D. J., Henze, D. K., and Seinfeld, J. H.: Effect of changes in climate and emissions on future sulfate-nitrate-ammonium aerosol levels in the United States, J. Geophys. Res., 114, D01205, doi:10.1029/2008JD010701, 2009.

590 Rienecker, M. M., Suarez, M. J., Todling, R., Bacmeister, J., Takacs, L., Liu, H.-C., Gu, W.,
591 Sienkiewicz, M., Koster, R. D., Gelaro, R., Stajner, I., and Nielsen, J. E.: The GEOS-5 Data
592 Assimilation System-Documentation of versions 5.0.1 and 5.1.0, and 5.2.0. NASA Tech. Rep.
593 Series on Global Modeling and Data Assimilation, NASA/TM-2008-104606, vol. 27, Goddard
594 Space Flight Center, Greenbelt, Maryland, USA, 92 p., 2008.
595
596 Ridley, D. A., Heald, C. L., Pierce, J. R., and Evans, M. J.: Toward resolution-independent dust
597 emissions in global models: Impacts on the seasonal and spatial distribution of dust, Geophys.
598 Res. Lett., 40, 2873–2877, doi:10.1002/grl.50409, 2013.
599
600 Rind, D., Lerner, J., Jonas, J., and McLinden, C.: Effects of resolution and model physics on
601 tracer transports in the NASA Goddard Institute for Space Studies general circulation models, J.
602 Geophys. Res., 112, D09315, doi:10.1029/2006JD007476, 2007.
603
604 Rotman, D. A., Atherton, C. S., Bergmann, D. J., Cameron-Smith, P. J., Chuang, C. C., Connel,
605 P. S., Dignon, J. E., Franz, A., Grant, K. E., Kinnison, D. E., Molenkamp, C. R., Proctor, D. D.,
606 and Tannahill, J. R.: IMPACT, the LLNL 3-D global atmospheric chemical transport model for
607 the combined troposphere and stratosphere: Model description and analysis of ozone and other
608 trace gases, J. Geophys. Res., 109, D04303, doi:10.1029/2002JD003155, 2004.
609
610 Santillana, M., Zhang, L., and Yantosca, R.: Estimating numerical errors due to operator splitting
611 in global atmospheric chemistry models: Transport and chemistry, J. Comput. Phys., 305, 372-
612 386, doi:10.1016/j.jcp.2015.10.052, 2016.
613
614 Shindell, D. T., Faluvegi, G., Stevenson, D. S., Krol, M. C., Emmons, L. K., Lamarque, J.-F.,
615 Petron, G., Dentener, F. J., Ellingsen, K., Schultz, M. G., Wild, O., Amann, M., Atherton, C. S.,
616 Bergmann, D. J., Bey, I., Butler, T., Cofala, J., Collins, W. J., Derwent, R. G., Doherty, R. M.,
617 Drevet, J., Eskes, H. J., Fiore, A. M., Gauss, M., Hauglustaine, D. A., Horowitz, L. W., Isaksen,
618 I. S. A., Lawrence, M. G., Montanaro, V., Muller, J. F., Pitari, G., Prather, M. J., Pyle, J. A.,
619 Rast, S., Rodriguez, J. M., Sanderson, M. G., Savage, N. H., Strahan, S. E., Sudo, K., Szopa, S.,
620 Unger, N., van Noije, T. P. C., and Zeng, G.: Multimodel simulations of carbon monoxide:
621 Comparison with observations and projected near-future changes, J. Geophys. Res., 111,
622 D19306, doi:10.1029/2006JD007100, 2006.
623
624 Sillman, S., Logan, J. A., and Wofsy, S. C.: A regional scale model for ozone in the United
625 States with subgrid representation of urban and power plant plumes, J. Geophys. Res., 95, 5731-
626 5748, doi:10.1029/JD095iD05p05731, 1990.
627
628 Sportisse, B.: An analysis of operator splitting techniques in the stiff case, J. Comput. Phys., 161,
629 140-168, doi:10.1006/jcph.2000.6495, 2000.
630
631 Strang, G.: On the construction and comparison of difference schemes, SIAM J. Numer. Anal., 5,
632 506-517, doi:10.1137/0705041, 1968.
633

Thompson, T. M., Saari, R. K., and Selin, N. E.: Air quality resolution for health impact assessment: influence of regional characteristics, Atmos. Chem. Phys., 14, 969-978, doi:10.5194/acp-14-969-2014, 2014.

van Donkelaar, A., Zhang, L., Chen, D., Martin, R. V., Pasch, A. N., Szykman, J. J., and Wang, Y. X.: Improving the accuracy of daily satellite-derived ground-level fine aerosol concentration estimates for North America, Environ. Sci. Technol., 46, 11971-11978, doi:10.1021/es3025319, 2012.

Valin, L. C., Russell, A. R., Hudman, R. C., and Cohen, R. C.: Effects of model resolution on the interpretation of satellite NO_2 observations, Atmos. Chem. Phys., 11, 11647-11655, doi:10.5194/acp-11-11647-2011, 2011.

Vinken, G. C. M., Boersma, K. F., Jacob, D. J., and Meijer, E. W.: Accounting for non-linear chemistry of ship plumes in the GEOS-Chem global chemistry transport model, Atmos. Chem. Phys., 11, 11707-11722, doi:10.5194/acp-11-11707-2011, 2011.

Wang, Q., Jacob, D. J., Fisher, J. A., Mao, J., Leibensperger, E. M., Carouge, C. C., Le Sager, P., Kondo, Y., Jimenez, J. L., Cubison, M. J., and Doherty, S. J.: Sources of carbonaceous aerosols and deposited black carbon in the Arctic in winter-spring: implications for radiative forcing, Atmos. Chem. Phys., 11, 12453-12473, doi:10.5194/acp-11-12453-2011, 2011.

Wang, H., Jacob, D. J., Le Sager, P., Streets, D. G., Park, R. J., Gilliland, A. B., and van Donkelaar, A.: Surface ozone background in the United States: Canadian and Mexican pollution influences, Atmos. Environ., 43, 1310–1319, doi:10.1016/j.atmosenv.2008.11.036, 2009.

Wang, Y., Jacob, D. J., and Logan, J. A.: Global simulation of tropospheric O_3-NO_x-hydrocarbon chemistry: 1. Model formulation, J. Geophys. Res., 103, 10713-10725, doi:10.1029/98JD00158, 1998.

Wang, Y. X., McElroy, M. B., Jacob D. J., and Yantosca, R. M.: A nested grid formulation for chemical transport over Asia: Applications to CO, J. Geophys. Res., 109, doi:10.1029/2004JD005237, 2004.

Wesely, M. L.: Parameterization of surface resistances to gaseous dry deposition in regional-scale numerical models, Atmos. Environ., 23, 1293-1304, doi:10.1016/0004-6981(89)90153-4, 1989.

Wild, O., and Prather, M. J.: Global tropospheric ozone modeling: Quantifying errors due to grid resolution, J. Geophys. Res., 111, D11305, doi:10.1029/2005JD006605, 2006.

Wu, S., Mickley, L. J., Jacob, D. J., Logan, J. A., Yantosca, R. M. and Rind, D.: Why are there large differences between models in global budgets of tropospheric ozone?, J. Geophys. Res., 112, D05302, doi:10.1029/2006JD007801, 2007.

Yan, Y.-Y., Lin, J.-T., Kuang, Y., Yang, D., and Zhang, L.: Tropospheric carbon monoxide over the Pacific during HIPPO: two-way coupled simulation of GEOS-Chem and its multiple nested models, Atmos. Chem. Phys., 14, 12649-12663, doi:10.5194/acp-14-12649-2014, 2014.

Yu, K., Jacob, D. J., Fisher, J. A., Kim, P. S., Marais, E. A., Miller, C. C., Travis, K. R., Zhu, L., Yantosca, R. M., Sulprizio, M. P., Cohen, R. C., Dibb, J. E., Fried, A., Mikoviny, T., Ryerson, T. B., Wennberg, P. O., and Wisthaler, A.: Sensitivity to grid resolution in the ability of a chemical transport model to simulate observed oxidant chemistry under high-isoprene conditions, Atmos. Chem. Phys. Discuss., doi:10.5194/acp-2015-980, in review, 2016.

Zender, C. S., Bian, H., and Newman, D.: The mineral dust entrainment and deposition (DEAD) model: description and 1990s dust climatology, J. Geophys. Res., 108, 4416, doi:10.1029/2002JD002775, 2003.

Zhang, L. M., Gong, S. L., Padro, J. and Barrie, L.: A size-segregated particle dry deposition scheme for an atmospheric aerosol module, Atmos. Environ., 35, 549-560, doi:10.1016/S1352-2310(00)00326-5, 2001.

Zhang, L., Jacob, D. J., Downey, N. V., Wood, D. A., Blewitt, D., Carouge, C. C., van Donkelaar, A., Jones, D. B. A., Murray, L. T., and Wang, Y.: Improved estimate of the policy-relevant background ozone in the United States using the GEOS-Chem global model with 1/2° × 2/3° horizontal resolution over North America, Atmos. Environ., 45, 6769-6776, doi:10.1016/j.atmosenv.2011.07.054, 2011.

723 Table 1: Comparison of mean* relative simulation error versus horizontal resolution, with "truth"

724 defined at 2^o x 2.5^o horizontal resolution

725

Species	Mean relative simulation error (unitless)	
	4^o x 5^o resolution	2^o x 2.5^o resolution
Nitrogen oxides	2.1	0.092
Secondary inorganic aerosols	1.0	0.14
Ozone	0.17	0.004
Carbon monoxide	0.36	0.005

726

727 * Mean taken for operator durations ≤ 30 min.

728

729

730

731

732

733

734

735

736

737

738

739

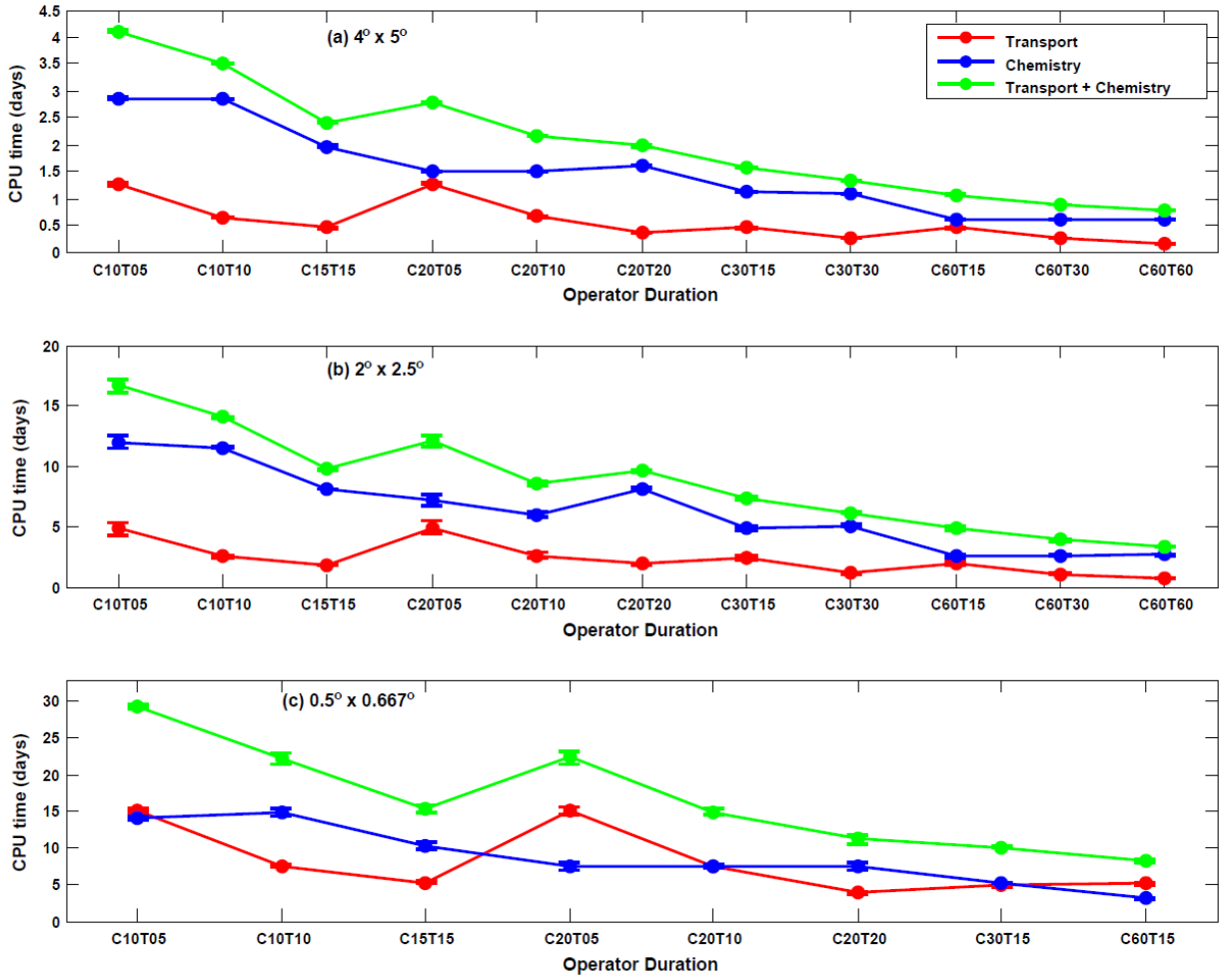

740

741 Figure 1: CPU time for GEOS-Chem simulations with various operator durations at three
742 horizontal resolutions. Global simulations are at 4° x 5° (top) and 2° x 2.5° (middle) resolutions.
743 The bottom panel contains results for the average of two nested regions North America and East
744 Asia at 0.5° x 0.667° resolution. Colored lines represent the CPU time for simulating transport (red)
745 and chemical (blue) operators, and the sum of the two (green). Error bars represent standard error
746 over five simulations. Simulations are represented in the abscissa as CccTtt with chemical operator
747 duration, C = cc minutes, and transport operator duration, T = tt minutes.

748

749

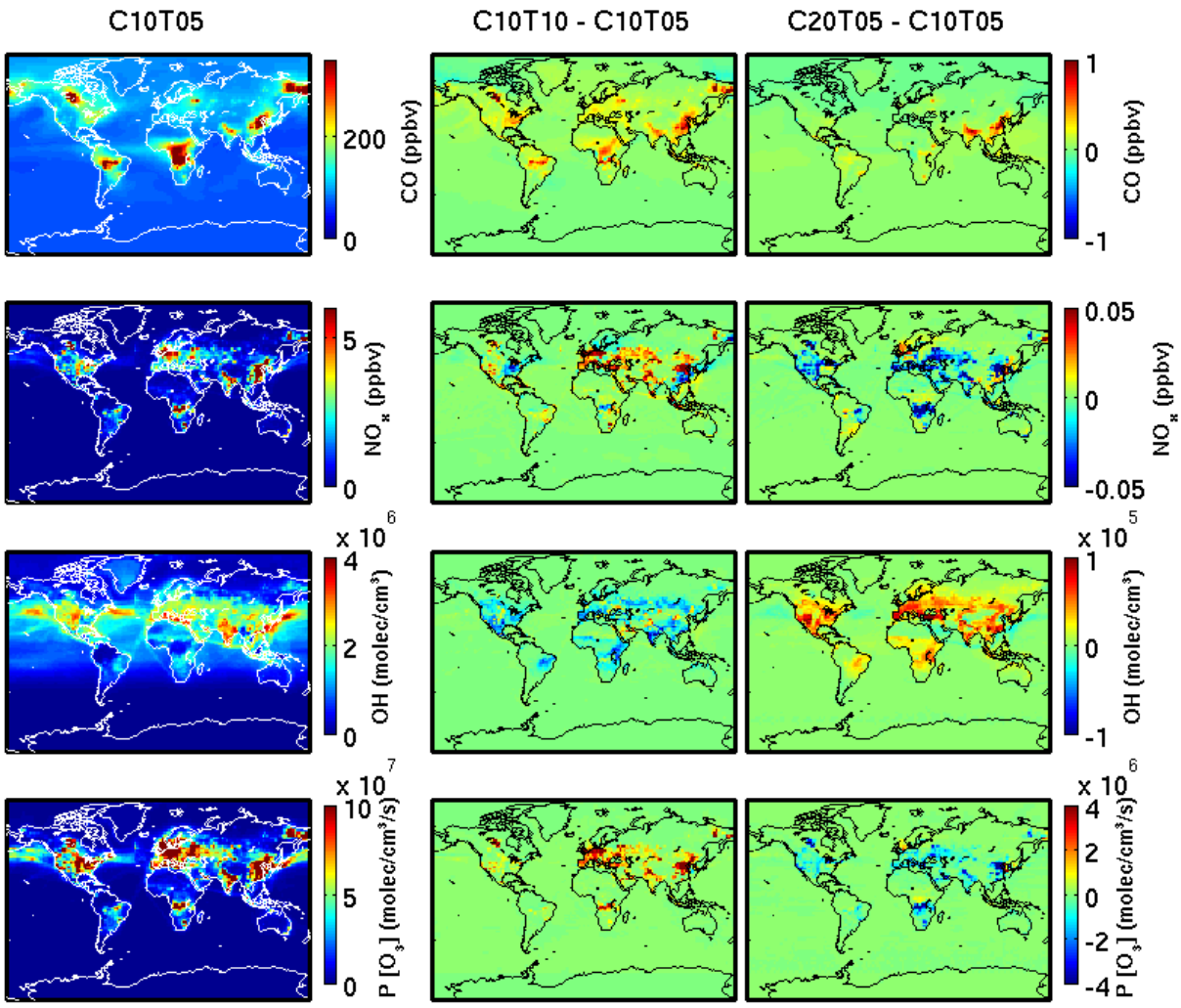

Figure 2a: Sensitivity of simulated species to the duration of chemical and transport operators. The left column contains monthly mean ground-level concentrations simulated with the shortest operator duration considered (C10T05) at 2º x 2.5º horizontal resolution. Other columns contain the absolute differences from doubling the transport operator duration to C10T10 (middle), and doubling the chemical operator duration to C20T05 (right). Each row from top to bottom represents carbon monoxide (CO), nitrogen oxides (NO_x), hydroxyl radical (OH), and the production of ozone (P[O3]). Simulations are represented as CccTtt with chemical operator duration, C = cc minutes, and transport operator duration, T = tt minutes.

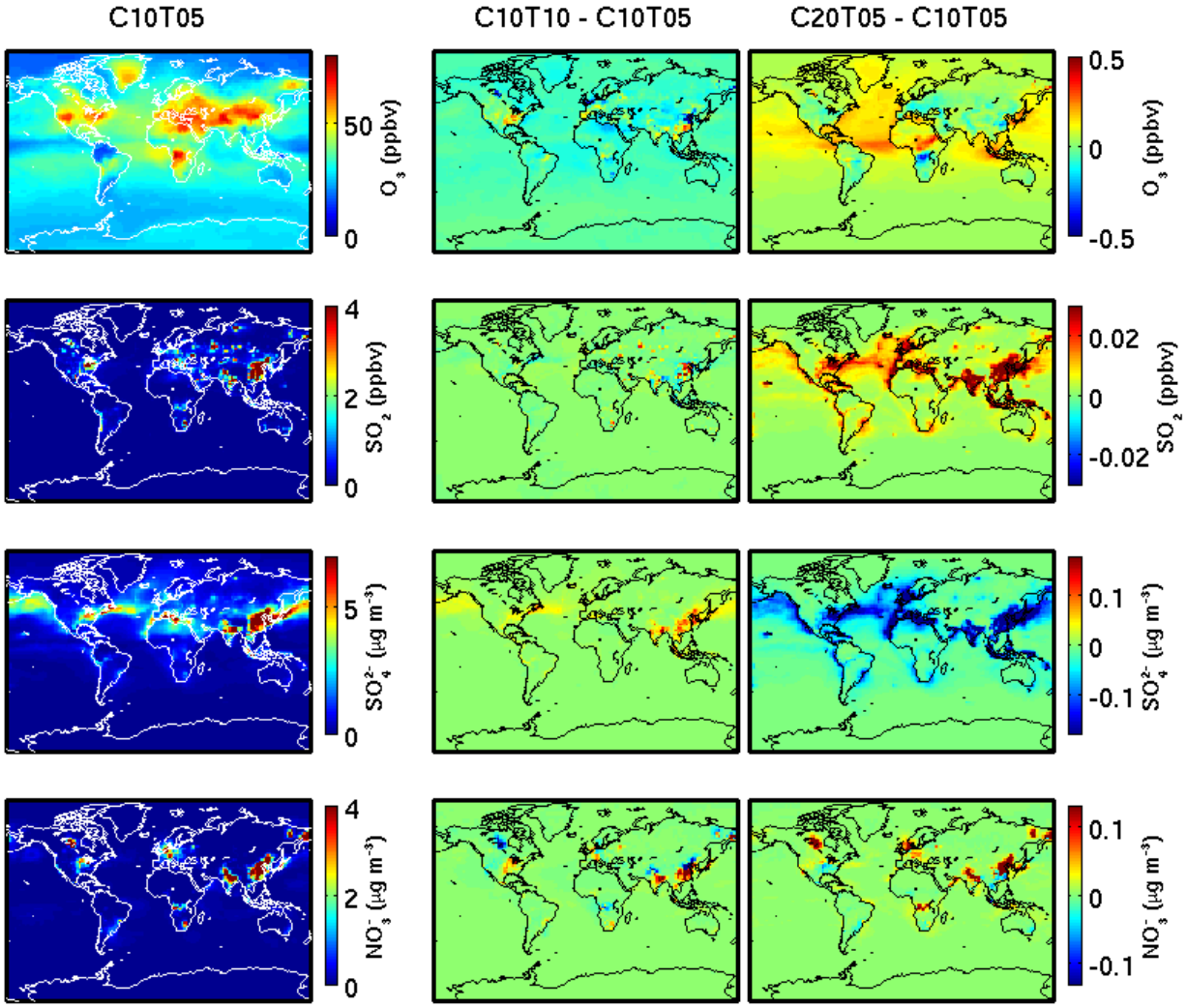

Figure 2b: As described in Fig. 2a, but each row from top to bottom represents ozone (O_3), sulfur dioxide (SO_2), sulfate (SO_4^{2-}), and nitrate (NO_3^-) respectively.

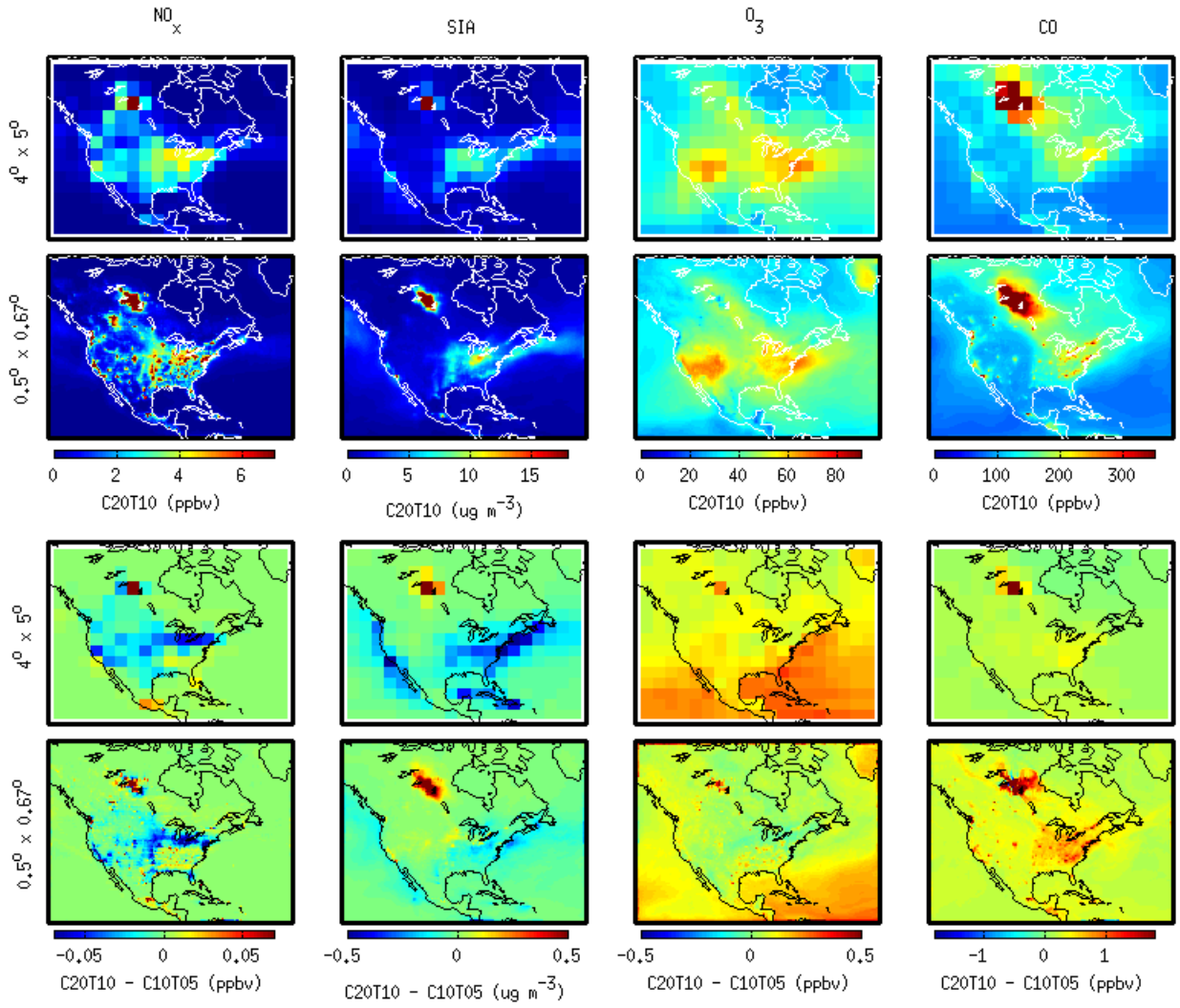

Figure 3: Sensitivity of simulated species to changes in operator duration (C20T10 to C10T05) at two different horizontal resolutions over North America (global 4^o x 5^o, and nested 0.5^o x 0.67^o simulations). The top two rows contain monthly mean ground-level concentrations simulated with the C20T10 operator duration for 4^o x 5^o (top row) and 0.5^o x 0.67^o (second row) resolutions. The two lowest rows contain the monthly mean differences (C20T10 minus C10T05) for 4^o x 5^o (third row) and 0.5^o x 0.67^o (bottom row) resolutions. Each column from left to right represents nitrogen oxides (NO_x), secondary inorganic aerosols (SIA), ozone (O_3), and carbon monoxide (CO).

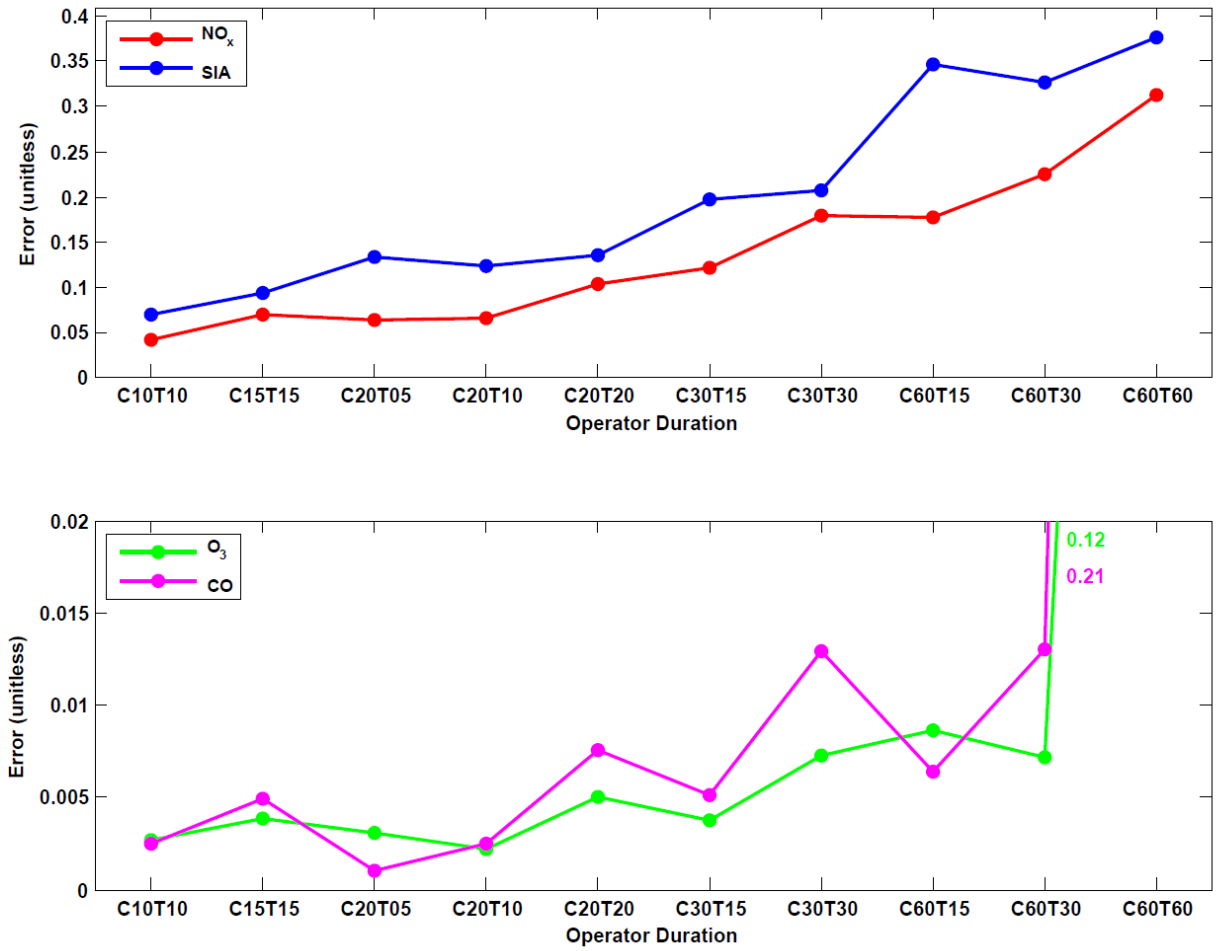

778

779 Figure 4: Relative simulation error of different species (E^{s}_{sim} , eq. 3) for GEOS-Chem with various

780 operator durations at 2º x 2.5º horizontal resolution. Colored lines and dots represent the relative

781 simulation error for nitrogen oxides (NO_x; red), secondary inorganic aerosols (SIA; blue), ozone

782 (O_3; green), and carbon monoxide (CO; magenta). Simulations are represented in the abscissa as

783 CccTtt with chemical operator duration, C = cc minutes, and transport operator duration, T = tt

784 minutes.

785

786

787

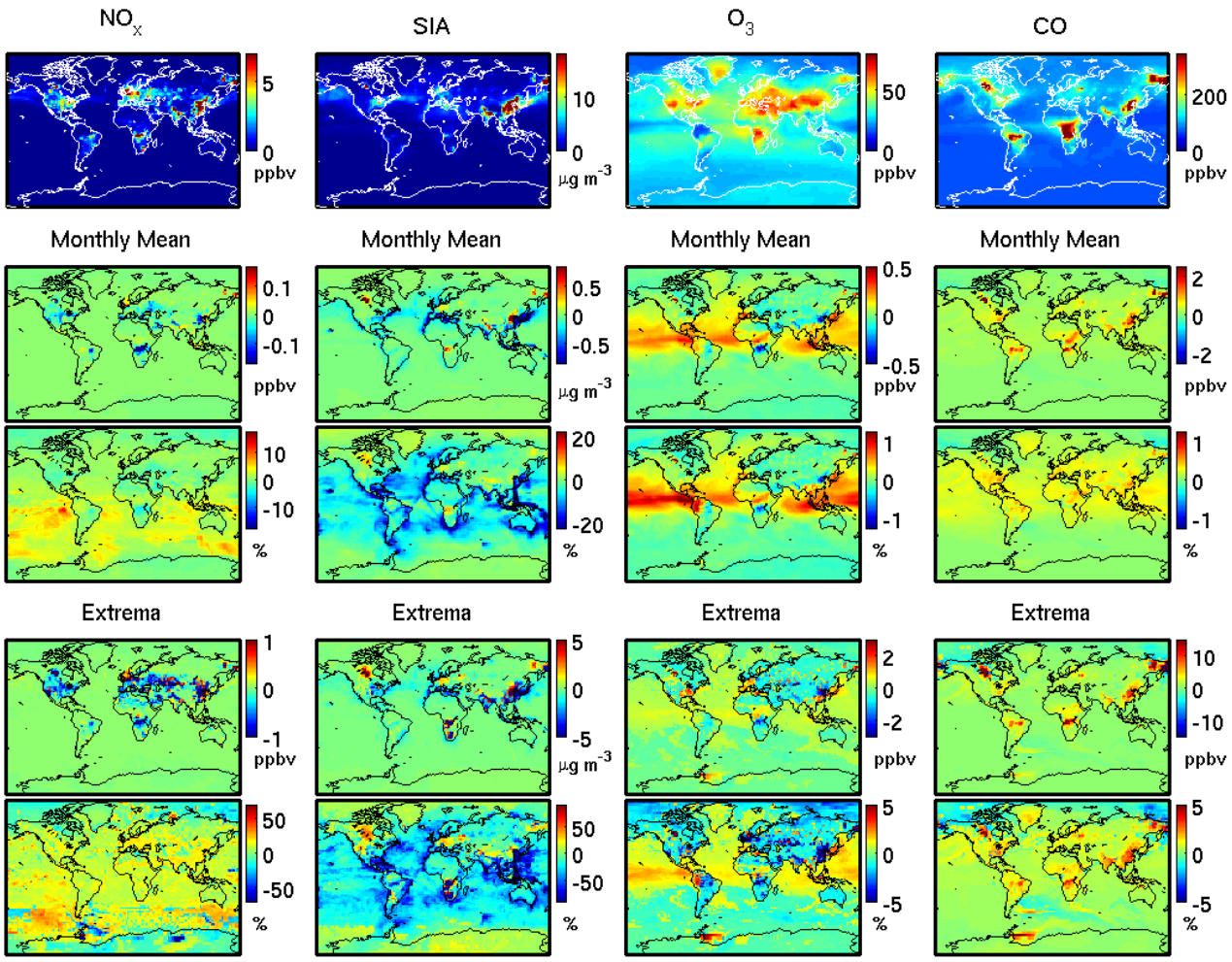

788

789

790 Figure 5: Effect on simulated species of changing from the GEOS-Chem traditional operator
791 durations (C30T15) to the shortest operator durations considered (C10T05). The top row contains
792 monthly mean ground-level concentrations simulated with the C30T15 operator duration at 2° x
793 2.5° horizontal resolution. The next two rows contain the monthly mean differences (C30T15
794 minus C10T05) for absolute (second row) and relative (third row) differences. The two lowest
795 rows contain the maximum differences (C30T15 minus C10T05) for absolute (fourth row) and
796 relative (bottom row) differences. Each column from left to right represents nitrogen oxides (NO_x),
797 secondary inorganic aerosols (SIA), ozone (O_3), and carbon monoxide (CO).

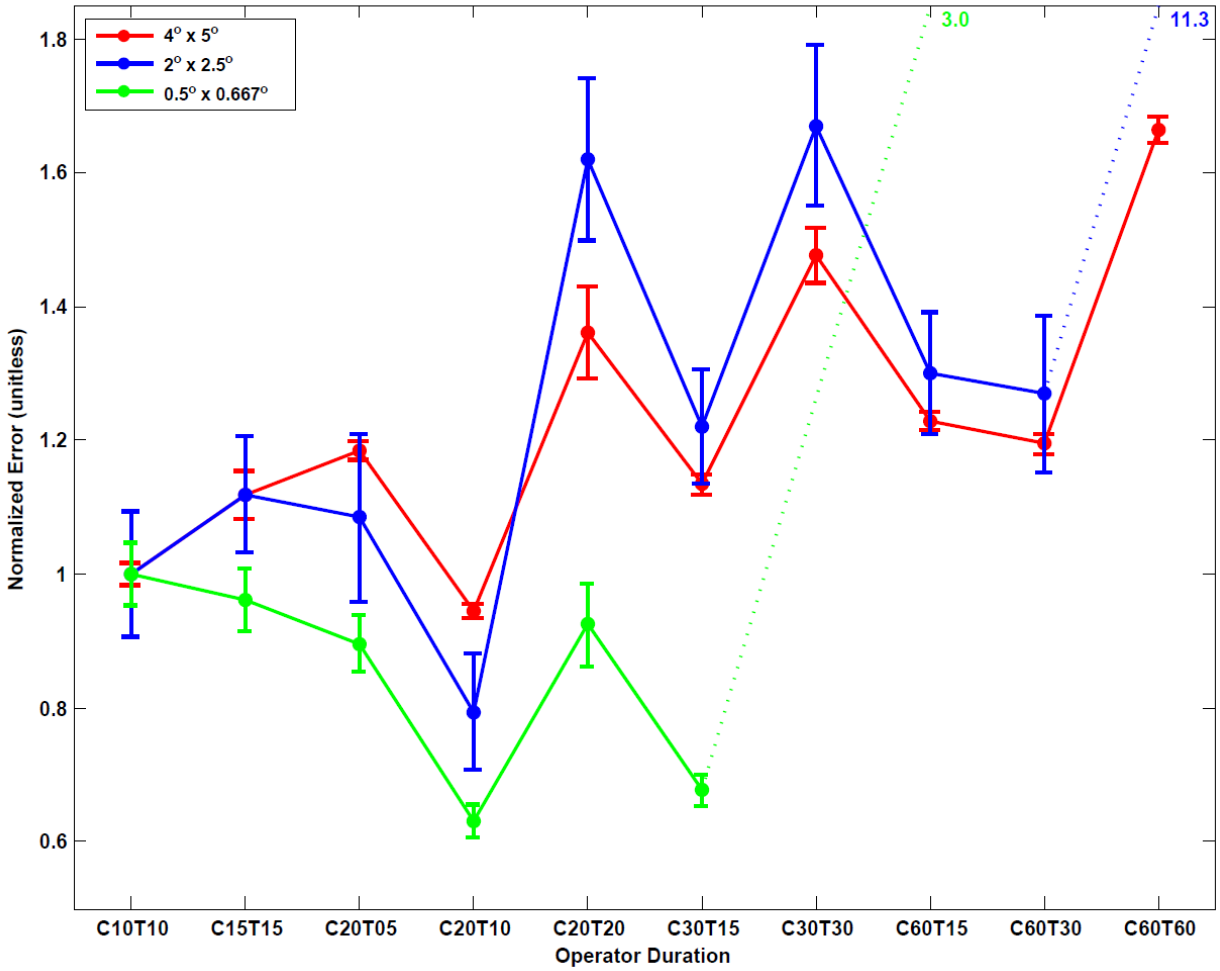

Figure 6: CPU-time adjusted Composite Normalized Error (CNE, eq. 4) for GEOS-Chem simulations with various horizontal resolutions and operator durations. Colored lines and dots represent the CNE for the global simulations at 4° x 5° (red) and 2° x 2.5° (blue), and the nested simulations at 0.5° x 0.667° (green) horizontal resolutions. Error bars represent standard error in CPU time. Simulations are represented in the abscissa as CccTtt with chemical operator duration, C = cc minutes, and transport operator duration, T = tt minutes.